Journal of
Synchrotron
Radiation

ISSN 1600-5775

Received 22 November 2013
Accepted 11 March 2014

08B1-1: an automated beamline for macromolecular crystallography experiments at the Canadian Light Source

Michel Fodje,[a,b]* Pawel Grochulski,[a,c] Kathryn Janzen,[a] Shaunivan Labiuk,[a] James Gorin[a] and Russ Berg[a]

[a]Canadian Light Source, 44 Innovation Boulevard, Saskatoon, Saskatchewan, Canada S7N2V3, [b]Biochemistry, University of Saskatchewan, 107 Wiggins Road, Saskatoon, Saskatchewan, Canada S7N5E5, and [c]College of Pharmacy and Nutrition, University of Saskatchewan, 110 Science Place, Saskatoon, Saskatchewan, Canada S7N5C9. *E-mail: michel.fodje@lightsource.ca

Beamline 08B1-1 is a recently commissioned bending-magnet beamline at the Canadian Light Source. The beamline is designed for automation and remote access. Together with the undulator-based beamline 08ID-1, they constitute the Canadian Macromolecular Crystallography Facility. This paper describes the design, specifications, hardware and software of beamline 08B1-1. A few scientific results using data obtained at the beamline will be highlighted.

Keywords: macromolecular crystallography; anomalous diffraction; mail-in crystallography; remote control; structural biology.

1. Introduction

The Canadian Light Source (CLS) is a third-generation synchrotron source located on the University of Saskatchewan campus in Saskatoon, Canada (Cutler *et al.*, 2007). The CLS has 12 straight sections (24 bending magnets), a circumference of 171 m and currently operates at an energy of 2.9 GeV with stored currents up to 250 mA. The construction and operation of the CLS has been funded by the Government of Canada, provincial governments, and academic and industrial partners. Beamline 08ID-1, the first Canadian Macromolecular Crystallography Facility (CMCF) beamline, was built during the first phase of construction together with the storage ring and went into operation in 2006 (Grochulski *et al.*, 2011), while beamline 08B1-1 has been built as part of the second phase of construction. Since the undulator-based 08ID-1 beamline was already available at CMCF to cater for weakly diffracting smaller crystals with larger unit cells, beamline 08B1-1 was designed to complement the existing capability with automation and remote access. For this purpose, ease-of-use and robustness were primary design objectives.

The design of beamline 08B1-1 started in 2006 and the beam was first observed at the sample position in July of 2009. Commissioning was completed in the fall of 2010 and the beamline was opened for general use in January of 2011. Together both CMCF beamlines serve a growing community of more than 60 research groups across Canada and USA.

2. Beamline overview

2.1. Optical design

The photon source for the beamline is the first bending magnet in the eighth straight-section, designated 08B1. A fixed-exit mask at the front-end provides an aperture limiting the beam to 1.5 mrad (horizontal) by 0.5 mrad (vertical), relative to the source point. The beamline acceptance can be reduced further by white-beam slits (WBS). The optical layout of the beamline consists of a vertical collimating mirror (VCM), a double-crystal monochromator (DCM) with Si(111) crystals, and a toroidal focusing mirror (TFM) (Fig. 1). The VCM is a flat-bent mirror made up of a single piece of silicon crystal with two reflective stripes, the first being a bilayer of rhodium coating over platinum while the second stripe is plain uncoated Si.

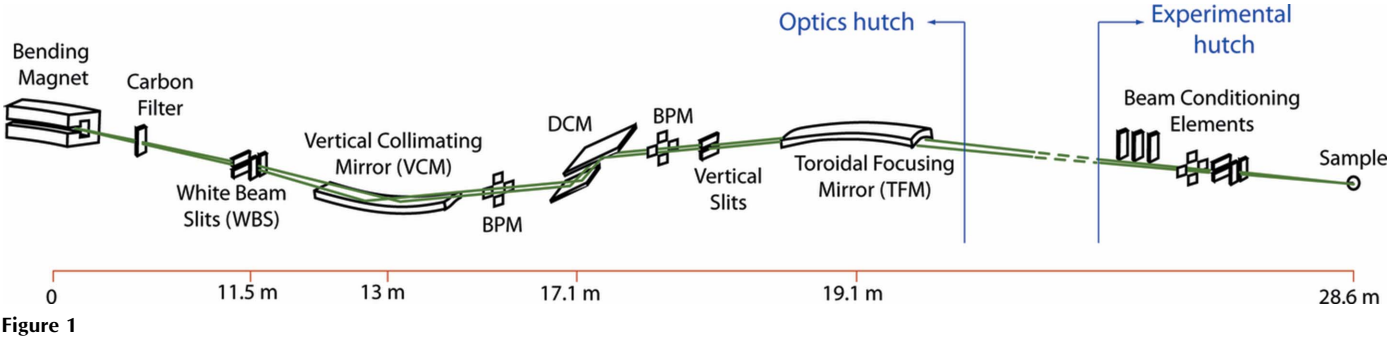

Figure 1
Schematic layout of the optical components of the CMCF 08B1-1 beamline showing distances of major components from the source, beam position monitors (BPM) and slits.

The DCM provides a tunable energy range of 4.0 to 18.0 keV with a fixed vertical offset of 32.5 mm. For better stability during energy changes, the second crystal of the DCM is 185 mm long and does not require translation along the beam during energy changes. In addition, the second crystal is equipped with a piezoelectric actuator used for automatic beam stabilization through a feedback controller. The TFM is a bent cylindrical mirror with fixed horizontal and adjustable vertical focal length. The mirror has a single reflective stripe coated with a bilayer of rhodium and platinum. It is well known that a toroidal mirror introduces aberrations due to the astigmatic nature of the source. However, under one condition an astigmatic toroidal mirror can produce reasonable image quality. This is accomplished with a TFM horizontal demagnification of 2:1 and by using the VCM to pre-collimate the beam in the vertical direction (MacDowell *et al.*, 2004). Beamline components such as the WBS and the first crystal of the DCM which come into contact with the white beam are water cooled.

For robustness and ease of use, each translation stage is equipped with a relative encoder containing a reference position. The absolute values of all reference positions were determined relative to the synchrotron coordinate system during beamline alignment and survey. In addition, mirror benders on the VCM and TFM are also fitted with force-sensing load-cells which allow safe recovery of the exact bending radius at all times.

The vaccum systems WBS, TFM and VCM including the benders were built by Johnsen Ultravac, Canada, while the DCM was supplied by Kohzu Precision, Japan. All optical substrates were supplied by Crystal Scientific, UK.

2.2. Experimental station

The end-station consists of beam-conditioning devices and a Maatel/EMBL MD2 microdiffractometer with MK3 mini-kappa mounted on a six-axis table (Bruker-AS) for alignment (Fig. 2). The monochromatic beam exiting a beryllium window upstream of the experimental enclosure can be attenuated using an XIA PF4 filter box fitted with aluminium foils of various thicknesses. Two quadrant diode beam position monitors (Bruker-AS) placed after the filter box, and alternating between two high-precision slits (JJ-X-ray), allow for accurate alignment of the end-station table. The conditioned beam travels through a fast electromagnetic shutter system (Bruker-AS) to the sample position at the MD2 microdiffractometer located 28.6 m from the source point. The MD2 provides on-axis sample visualization, an air-bearing goniometer equipped with an MK3 mini-kappa head, integrated beam-shaping apertures and built-in synchronization of the fast shutter with goniometer rotation during data collection. The MD2 is also fitted with a Maatel/EMBL movable beamstop. The sample environment is cooled using an Oxford Instruments Cryojet XL system. Alternatively the Cryojet nozzle can be replaced on request with a Maatel/EMBL humidity control device (HC1) in order to perform controlled dehydration experiments at room temperature. A Bruker XFlash 410 Si-drift detector is permanently mounted on the MD2 and is pneumatically translated close to the sample for MAD scans and X-ray excitation and fluorescence experiments. In addition, a Vortex ME4 multi-element fluorescence detector (Hitachi) is also available for performing EXAFS experiments on protein crystals. The end-station is also equipped with a Stanford-type automounter (SAM) which accepts either SSRL cassettes or universal pucks and can hold up to 288 samples at a time (Cohen *et al.*, 2002). A high-speed barcode reader (Quadrus MINI Velocity, Microscan), installed close to the SAM, allows reading of data matrix codes on sample pins during mounting. Diffraction data

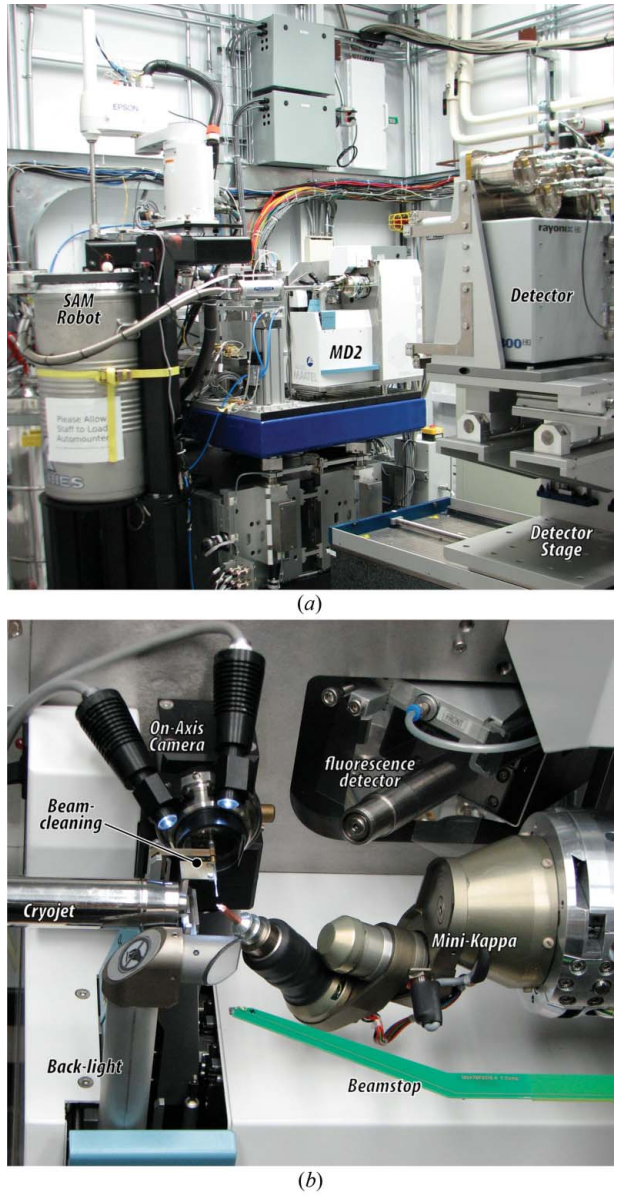

Figure 2
(*a*) Photographs of the end-station components showing the SAM robot, CCD detector and MD2 microdiffractometer with MK3 mini-kappa and (*b*) a close-up view of the sample position.

are collected using a Rayonix MX300HE CCD detector mounted on a three-axis support stage (Bruker-AS) which allows the sample-to-detector distance to be varied between 110 and 800 mm and a maximum 'swing-up' 2θ angle of 20°. The beamline parameters are presented in Table 1.

3. Ancillary facilities

3.1. Software

The low-level beamline control system is based on the Experimental Physics and Industrial Control System (EPICS) (Dalesio *et al.*, 1994). EPICS calibration routines were written in State-Notation-Language (SNL) to permit calibration of all stages using the encoder reference signals. For controlling the SAM automounter, EPICS interfaces are provided to the original *Blu-ICE/DCSS* software

Table 1
Beamline details.

Beamline name	08B1-1
Source type	Bending magnet
Mirrors	1m VCM Si with Rh/Pt and Si stripes, 1 m toroid with Rh/Pt coating
Monochromator	Water-cooled DCM with Si(111) crystals
Energy range (keV)	4–18.0
Wavelength range (Å)	3.1–0.69
Beam size (uncollimated, FWHM) (μm)	230 × 180
Beam size (collimated, typical) (μm)	200
Flux (at 12 keV, 250 mA) (photons s^{-1})†	1.5×10^{11}
Goniometer	MD2 microdiffractometer with MK3 mini-kappa
Cryo capability	95–300 K, LN_2 cryojet
Sample mounting	SAM automounter
Detector type	CCD
Detector model	Rayonix MX300HE
2θ capabilities	0–20°

† Measured using a calibrated ion chamber placed close to the sample position.

(McPhillips *et al.*, 2002) which is used directly only for calibrating and configuring the automounter. End-user software consists of *MxDC* and *MxLIVE* for data collection and experiment management (Fodje *et al.*, 2012). *MxDC* provides automated sample mounting and centring, automated screening of multiple samples and automated analysis of X-ray fluorescence spectra. The software also allows automated tracking and verification of samples using barcodes. *MxDC* and *MxLIVE* are both integrated with an in-house-developed automatic screening and data processing pipeline known as *AutoProcess*. *AutoProcess* is written in Python and is based on the *XDS* data-processing package (Kabsch, 1993), *POINTLESS* (Evans, 2006), *BEST* (Bourenkov & Popov, 2006), *XDSSTAT* (Diederichs, 2006) and the *CCP4* package (Winn *et al.*, 2011). *AutoProcess* also uses *XTRIAGE* from *PHENIX* (Adams *et al.*, 2010) for data quality assessment. *AutoProcess* can be used directly from the *MxDC* interface. Graphical reports of the results are also displayed within *MxDC* and *MxLIVE*.

Other data processing/analysis packages commonly used by crystallographers are available, such as *HKL2000*, *MOSFLM*, *PHENIX*, *SHELX* and *COOT*. Remote access to the beamline is achieved through the *NoMachine NX* software package (NoMachine, Luxembourg).

3.2. User area and computing facilities

Users of the 08B1-1 beamline have access to a comfortable work-area for controlling their experiments and performing data analysis. In addition, a Dewar storage room and a sample preparation room are available close to the experimental enclosure. CMCF users also have access to a wet laboratory not far from the beamline (Fig. 3).

In addition to the workstations available in the control area, a 128 Core compute cluster with 15 TB of short-term and 30 TB of long-term storage is shared between both CMCF beamlines. The cluster allows fast concurrent data processing through the *AutoProcess* pipeline. Data transfer is primarily through portable USB hard drives brought by users; however, users are also able to download full datasets and processed results through the *MxLIVE* system. A DVD/Blu-ray disc-burning robot is also available.

4. Facility access

Access to the beamline can either be through a peer-reviewed general user program or through a fee-for-service program. At least 55% of available beam time is devoted to the peer-reviewed programs while up to 25% is reserved for commercial usage. The rest of the time is devoted to beamline maintenance and for use by beamline staff. New proposals are peer-reviewed twice a year and scored based on scientific merit and beamline suitability. Approved proposals remain active for two years during which users can request beam time at least two weeks in advance of the desired date. Beamline staff schedule beam time requests based on availability, giving priority to the highest scored proposals. Users are scheduled on one of the CMCF beamlines based on the type of experiment being performed and on the quality of their crystals. Thus, users with small weakly diffracting crystals or large unit cells, who need a brighter beam, are scheduled on the 08ID-1 beamline, while users with relatively large crystals who need repeated measurements for purposes such as ligand and fragment screening are scheduled on the 08B1-1 beamline. A mail-in service is also offered to the highest-ranked proposals. The data are collected by experienced CMCF staff according to instructions provided by the investigators.

Remote access is available after suitable training which can be provided remotely for users with previous synchrotron experience.

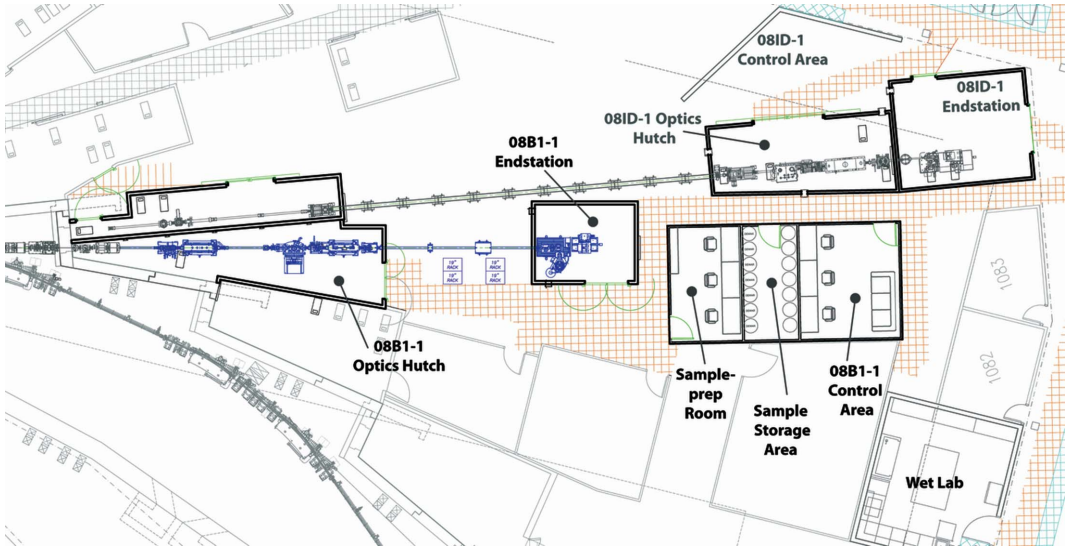

Figure 3
Plan of sector 8 at the Canadian Light Source, showing beamlines 08B1-1, 08ID-1 and ancillary facilities. The 08B1-1 beamline components are highlighted in blue.

Alternatively, the CMCF organizes a week-long synchrotron data-collection school in the summer every year, during which participants are provided with required training to be able to operate the beamlines remotely. Since the start of general operations in 2011, about 50% of users have been remote. Further details about remote-access procedures and training programs are available at the beamline website (http://cmcf.lightsource.ca).

5. Highlights

Beamline 08B1-1 was officially opened for general peer-review access in January 2011. Since then, data from the beamline have contributed to several Protein Data Bank (PDB) depositions and scientific articles. Up-to-date statistics of beamline output can be found in the BioSync database (Kuller *et al.*, 2001) which tracks non-commercial scientific output from macromolecular crystallography beamlines. A few scientific highlights of results obtained at the beamline are presented below.

5.1. MAD/SAD: small RNA sorting in plants

Small RNA molecules such as (mi)RNAs and (si)RNAs, typically 20 to 30 nucleotides long, occur naturally in eukaryotic cells and are critical during the regulation of many cellular processes. These small RNAs associate with argonaute proteins to form the RNA-induced silencing complex which serves to silence gene expression through a number of methods, including chromosomal modifications and post-transcriptional effects. Using SeMet SAD data collected at beamline 08B1-1 through the CMCF 'Mail-In' program, researchers were able to solve the structure of the MID domain of an *Arabidopsis thaliana* argonaute protein, AGO1(Fig. 4, PDB code 4g0x), to a resolution of 1.35 Å (Frank *et al.*, 2012).

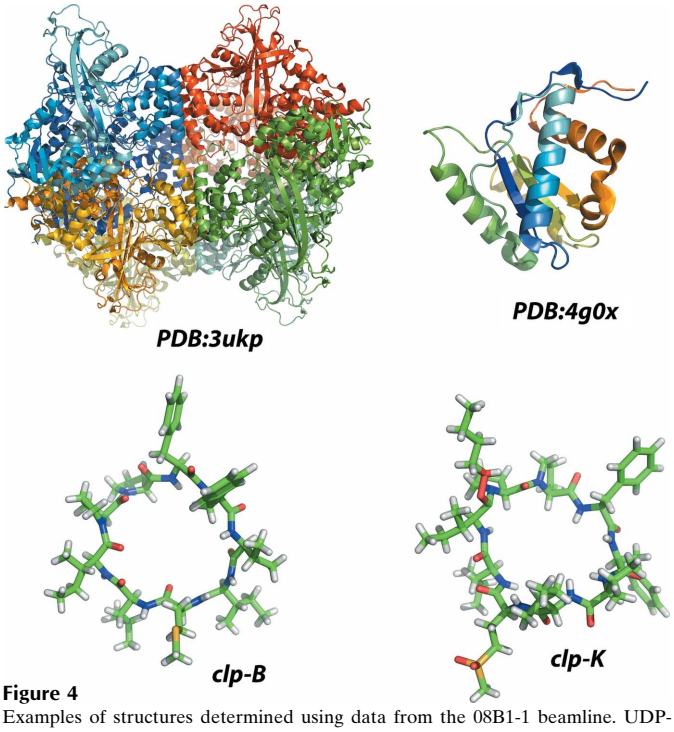

Figure 4
Examples of structures determined using data from the 08B1-1 beamline. UDP-galactopyranose mutase from *Aspergillus fumigatus* (PDB code 3ukp). *Arabidopsis thaliana* argonaute protein, AGO1 (PDB code 4g0x). Flaxseed cyclolinopeptide B methanol trisolvate (clp-B) and cyclolinopeptide K butanol disolvate monohydrate (clp-K). Figures were created using *PyMOL* (Schrödinger, LLC).

5.2. High-resolution: cyclolinopeptides

Along with high contents of triglyceride oil, flaxseed contains lignans and small amounts of hydrophobic cyclolinopeptides. The cyclolinopeptide entities have attracted recent attention because of their potential biological activities, including immuno-suppressive effects among others. Two high-resolution cyclolinopeptide structures have been determined using data from beamline 08B1-1 (Fig. 4). Cyclolinopeptide-K was determined to a resolution of 0.77 Å (Jadhav *et al.*, 2011) and cyclolinopeptide-B to a resolution of 0.75 Å (Schatte *et al.*, 2012). The presence of 2θ offset and mini-kappa capabilities on the beamline allowed complete and good quality data to be collected on crystals of these relatively small biomolecules.

5.3. UDP-galactopyranose mutase

UDP-galactopyranose mutase (UGM) catalyses the biosynthesis of galactofuranose, an important cell-wall component of several pathogenic microorganisms such as *Mycobacterium tuberculosis* and *Aspergillus fumigatus*. Since UGM is not expressed in humans and galactofuranose is not a normal component of the human body, UGM is a potential target for drug design. Using data obtained on both beamlines 08B1-1 and 08ID-1 and processed with *AutoProcess*, researchers determined the first eukaryotic UGM structures from *A. fumigatus* in unliganded UDP-galactopyranose-bound (Fig. 4, PDB code 3ukp) and UDP-bound forms (van Straaten *et al.*, 2012). These results highlight the use of the *AutoProcess* data-processing pipeline for automated data processing.

6. Discussion and conclusions

Beamline 08B1-1, one of the CMCF beamlines at the Canadian Light Source, has been in operation since 2010 complementing the existing beamline 08ID-1. To achieve the goal of robustness, the design incorporated features to permit reliable recovery of beamline parameters using encoders and calibration routines. In addition, the use of a long second crystal in the DCM together with feedback-controlled beam stabilization allows for a stable beam during experiments at fixed energy as well as automated beam delivery at any user-requested energy.

The user software environment which consists of *MxDC*, *MxLIVE* and *AutoProcess* together provide an integrated user-friendly and experiment-focused environment for synchrotron macromolecular crystallography. Combined with the SAM automounter, which can hold up to 288 samples at a time, the system automates many of the tasks traditionally performed manually and provides users with live beamline diagnostic information so that users can troubleshoot beamline problems remotely. For remote users, appropriate training is provided remotely and, except for the loading of samples into the robot and securing the hutch, which are performed by staff, all other steps required for running the experiment are carried out remotely through the user-friendly *MxDC* and *MxLIVE* interfaces without any staff intervention. Data collection is now routinely performed by both remote and local users from across North America, with each category accounting for about 50% of used beam-time.

Additional capabilities such as controlled dehydration at room temperature using a humidity control device (Sanchez-Weatherby *et al.*, 2009) and EXAFS scans on metalloprotein crystals are also available (Cotelesage *et al.*, 2012). Future developments in progress include an online UV/visible spectrometry system for monitoring photochemical reactions in crystals during data collection and the capability to perform diffraction anomalous fine-structure (DAFS) experiments (Stragier *et al.*, 1992).

The authors are grateful to Aina Cohen, Jinhu Song and other staff of the MX group at SSRL for assistance during the implementation and commissioning of the SAM Automounter. Additionally we would like to thank the CMCF Beamline Advisory Team for their support and guidance. The Canadian Light Source is funded by the Natural Sciences and Engineering Research Council of Canada, the National Research Council of Canada, the Canadian Institutes of Health Research, the Province of Saskatchewan, Western Economic Diversification Canada, and the University of Saskatchewan.

References

Adams, P. D., Afonine, P. V., Bunkóczi, G., Chen, V. B., Davis, I. W., Echols, N., Headd, J. J., Hung, L.-W., Kapral, G. J., Grosse-Kunstleve, R. W., McCoy, A. J., Moriarty, N. W., Oeffner, R., Read, R. J., Richardson, D. C., Richardson, J. S., Terwilliger, T. C. & Zwart, P. H. (2010). *Acta Cryst.* D**66**, 213–221.

Bourenkov, G. P. & Popov, A. N. (2006). *Acta Cryst.* D**62**, 58–64.

Cohen, A. E., Ellis, P. J., Miller, M. D., Deacon, A. M. & Phizackerley, R. P. (2002). *J. Appl. Cryst.* **35**, 720–726.

Cotelesage, J. J., Pushie, M. J., Grochulski, P., Pickering, I. J. & George, G. N. (2012). *J. Inorg. Biochem.* **115**, 127–137.

Cutler, J., Hallin, E., de Jong, M., Thomlinson, W. & Ellis, T. (2007). *Nucl. Instrum. Methods Phys. Res. A*, **582**, 11–13.

Dalesio, L. R., Hill, J. O., Kraimer, M., Lewis, S., Murray, D., Hunt, S., Watson, W., Clausen, M. & Dalesio, J. (1994). *Nucl. Instrum. Methods Phys. Res. A*, **352**, 179–184.

Diederichs, K. (2006). *Acta Cryst.* D**62**, 96–101.

Evans, P. (2006). *Acta Cryst.* D**62**, 72–82.

Fodje, M., Janzen, K., Berg, R., Black, G., Labiuk, S., Gorin, J. & Grochulski, P. (2012). *J. Synchrotron Rad.* **19**, 274–280.

Frank, F., Hauver, J., Sonenberg, N. & Nagar, B. (2012). *EMBO J.* **31**, 3588–3595.

Grochulski, P., Fodje, M. N., Gorin, J., Labiuk, S. L. & Berg, R. (2011). *J. Synchrotron Rad.* **18**, 681–684.

Jadhav, P., Schatte, G., Labiuk, S., Burnett, P.-G., Li, B., Okinyo-Owiti, D., Reaney, M., Grochulski, P., Fodje, M. & Sammynaiken, R. (2011). *Acta Cryst.* E**67**, o2360–o2361.

Kabsch, W. (1993). *J. Appl. Cryst.* **26**, 795–800.

Kuller, A., Fleri, W., Bluhm, W. F., Bourne, P. E., Smith, J. L. & Westbrook, J. (2001). *Nat. Struct. Mol. Biol.* **8**, 663.

MacDowell, A. A., Celestre, R. S., Howells, M., McKinney, W., Krupnick, J., Cambie, D., Domning, E. E., Duarte, R. M., Kelez, N., Plate, D. W., Cork, C. W., Earnest, T. N., Dickert, J., Meigs, G., Ralston, C., Holton, J. M., Alber, T., Berger, J. M., Agard, D. A. & Padmore, H. A. (2004). *J. Synchrotron Rad.* **11**, 447–455.

McPhillips, T. M., McPhillips, S. E., Chiu, H.-J., Cohen, A. E., Deacon, A. M., Ellis, P. J., Garman, E., Gonzalez, A., Sauter, N. K., Phizackerley, R. P., Soltis, S. M. & Kuhn, P. (2002). *J. Synchrotron Rad.* **9**, 401–406.

Sanchez-Weatherby, J., Bowler, M. W., Huet, J., Gobbo, A., Felisaz, F., Lavault, B., Moya, R., Kadlec, J., Ravelli, R. B. G. & Cipriani, F. (2009). *Acta Cryst.* D**65**, 1237–1246.

Schatte, G., Labiuk, S., Li, B., Burnett, P.-G., Reaney, M., Grochulski, P., Fodje, M., Yang, J. & Sammynaiken, R. (2012). *Acta Cryst.* E**68**, o50–o51.

Straaten, K. E. van, Routier, F. H. & Sanders, D. A. (2012). *J. Biol. Chem.* **287**, 10780–10790.

Stragier, H., Cross, J. O., Rehr, J. J., Sorensen, L. B., Bouldin, C. E. & Woicik, J. C. (1992). *Phys. Rev. Lett.* **69**, 3064–3067.

Winn, M. D., Ballard, C. C., Cowtan, K. D., Dodson, E. J., Emsley, P., Evans, P. R., Keegan, R. M., Krissinel, E. B., Leslie, A. G. W., McCoy, A., McNicholas, S. J., Murshudov, G. N., Pannu, N. S., Potterton, E. A., Powell, H. R., Read, R. J., Vagin, A. & Wilson, K. S. (2011). *Acta Cryst.* D**67**, 235–242.